

Fermi surface and electronic structure of ordered Cu_3Au

P. P. Deimel, R. J. Higgins, and R. K. Goodall

Physics Department, University of Oregon, Eugene, Oregon 97403

(Received 18 May 1981; revised manuscript received 31 July 1981)

The Fermi surface of ordered Cu_3Au , measured by de Haas–van Alphen spectroscopy, explains why the Hall coefficient changes sign, and displays a topology in excellent agreement with a recent band calculation. A direct measurement of the neck radius in this concentrated alloy is in surprising agreement with the rigid-band value. The superlattice band gap is approximately 0.04 Ry. Since large portions of the Fermi surface are close to the superlattice zone planes, the electronic contribution to the order-disorder transformation is non-negligible.

The Fermi surface (FS) of ordered Cu_3Au has long been thought to be qualitatively different from the FS of the noble metals. The Hall coefficient changes sign on ordering¹; other physical properties show singularities.² The long-period superlattice in CuAu is thought to originate in FS nesting as in charge-density wave systems.³ Although the superlattice in Cu_3Au is commensurate, the ordering process is accomplished by the growth of quantized $\sim 50 \text{ \AA}$ domains.⁴ A recent calculation⁵ predicts the same T_c for both Cu_3Au and Au_3Cu ; however, the measured T_c is about 200 K higher for Cu_3Au . These results suggest an electronically driven contribution to the phase transformation, similar to the charge-density-wave superlattices in layer compounds of recent interest.⁶ The Cu_3Au system has the advantage that the band structure of the constituents is well known, and not subject to huge variation in FS with slight variations in E_F , as in the transition-metal layer compounds. A recent band calculation⁷ shows features which could explain the anomalous changes in electronic properties of Cu_3Au , but no previous FS measurements were available to compare with.

The dominant effects are visible by examining in Fig. 1 the zero-gap, coherent-potential, or rigid-band FS, calculated from weighted FS expansions⁸ for the pure metals. Band 2, when remapped into the smaller simple cubic Brillouin zone (BZ), is a large hole sheet, consistent with the change in sign of the Hall effect. There are large flat regions near superlattice zone planes which could drive a charge-density-wave-like mechanism for ordering. In this Communication, we report data and interpretations which focus on two features; orbits which encompass the noble-metal neck region [R in Fig. 1(b)] are a measure of band structure in a concentrated alloy; orbits which cross superlattice zone faces only [Fig. 1(a)] are a measure of the electronic contribution to ordering.

Previous attempts to measure the FS of Cu_3Au by the de Haas–van Alphen (dHvA) effect were unsuccessful. One must simultaneously control stoichiometry, and reach large values of the long-

range order parameter, S , and the ordered domain size, d . From transport measurements, it is known that both S and d influence the scattering and the qualitative features of the Hall effect and thermopower.² The present experiment was the successful result of a carefully designed crystal growth and an-

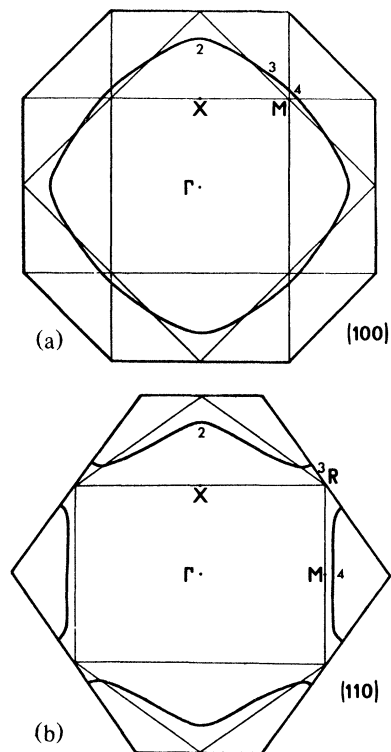


FIG. 1. Zero-gap coherent-potential, or rigid-band Fermi surface for Cu_3Au . The surface is calculated from the weighted average of Halse's expansion (Ref. 8), with coefficients derived from the experimental FS of Cu and Au. Band labelings 2, 3, and 4 are for the FS remapped into the Cu_3Au Brillouin zone. The labeling of points in the zone is for the simple cubic (ordered) Brillouin zone, for comparison with Fig. 3.

nealing strategy lasting more than 1 yr.^{9,10}

A portion of the results (Fig. 2) shows orbits in three main groups, from 10 to 45 MG. The topology is consistent with the FS calculated recently⁸ and shown in Fig. 3. The second-band holes form a closed, almost cubelike sheet. The third-band electrons form an open "jungle gym." The fourth-band electrons form an octahedron with bumps along [100]; this sheet is pinched off by the superlattice gap from the open jungle gym of the zero-gap model [Fig. 1(b), label 4]. A more detailed experimental FS topology and justification for this identification will be discussed separately.¹⁰ We compare calculated areas in the (100) plane of Fig. 3 with experiment (orbits measured with \vec{H} along [100]). The units are scaled to the length of the cube edge of the Brillouin zone in the ordered structure. The agreement is satisfactory, with the pointed third-band sheet more rounded off than the band-calculation prediction.

We concentrate here on interpreting two rather distinct features which appear in the remapped FS of Fig. 3: (a) The concentrated alloy band structure of the "neck" region of Fig. 1 appears near the point R ; (b) the superlattice band gap splits the third-band

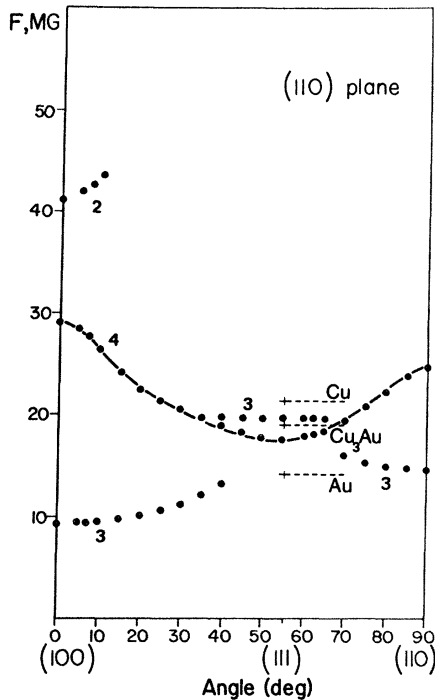


FIG. 2. Measured dHvA frequencies in the (110) plane of Cu_3Au . The band identification corresponds to that of Fig. 3. The solid curve is a fit with cubic polynomials from which the k vectors of this closed sheet have been calculated (Refs. 10 and 11). Also shown are the neck frequencies of Cu and Au and their weighted average.

TABLE I. Areas in the (100) plane.

Area $(2\pi/A)^{-2}$	Expt.	Theor.
Second-zone holes	0.141	0.158
Third-zone electrons	0.031	0.053

electrons from the second-band holes and is most clearly observable along the $\Gamma - M$ line.

a. Concentrated alloy band structure. The region near R on both the third- and fourth-band sheets originates near the neck on the Cu-like unremapped FS. In fact, the radius vectors shown along $X-R$ map back to the neck in the fcc BZ, and are thus a measure of the neck radius k_N in the concentrated alloy. Shown on Fig. 2 for comparison is the weighted average of Cu and Au neck areas. The agreement with the average of band 3 and 4 areas is remarkable.¹¹ The neck of Cu_3Au is almost a linear combination of Cu and Au necks—surprisingly "rigid-band" behavior.

b. Superlattice band gap. We now look at orbits dominated by superlattice Bragg reflections. The splitting shown in Fig. 3 along the $\Gamma - M$ line is a measure of the superlattice band gap, E_G . To estimate E_G , suppose that

$$A(\text{CPA}) - A(\text{obs}) = A(\text{NFE}) - A(\text{OPW}) \quad (1)$$

To estimate the amount by which the actual areas,

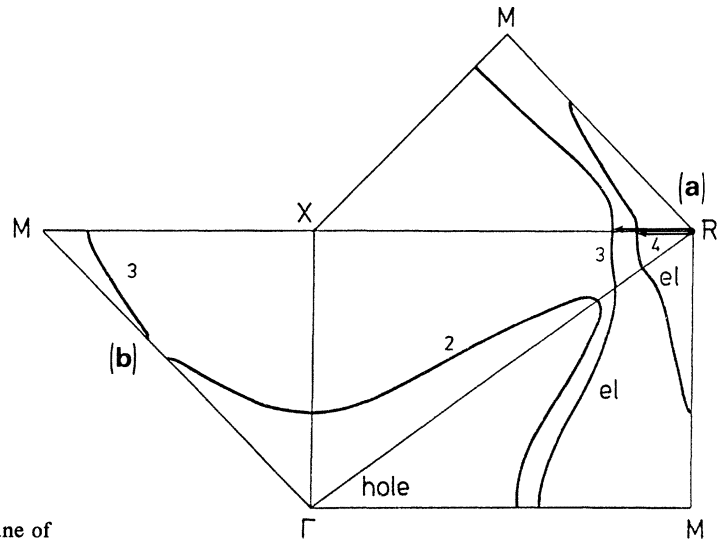


FIG. 3. Cu_3Au Fermi surface predicted from the band calculation of Ref. 8. The band labeling is as in Figs. 1 and 2. We focus in this Communication on the regions labeled (a) and (b).

TABLE II. Comparison of F values.

	F (10^6 G)
Expt. average $(F_3 + F_4)/2$	~ 18.5
Predicted neck $[3F_N(\text{Cu}) + 1F_N(\text{Au})]/4$	~ 20.1
Band calculation (Ref. 7) (band 3 + band 4)/2	16.0

A (obs) (Fig. 3 as measured by the data of Fig. 2) are shrunk by the superlattice gap from the coherent potential cross sections (zero gap, Fig. 1), the orbits of a Harrison construction nearly-free-electron FS, A (NFE), are shrunk by turning on the band gaps in first-order perturbation theory [A (OPW)] until the equation balances. The comparison is limited to second-zone holes and third-zone electrons in the (100) plane, for which the connection with a NFE FS is recognizable, and the stronger lattice potential contributions tend to cancel by difference in Eq. (1). A (CPA) (CPA is the coherent potential approximation) was obtained from a weighted sum of Cu and Au FS with the Fourier coefficients due to Halse,⁸ with the lattice constant adjusted to the correct value for Cu_3Au .

The band-gap estimate we obtain from Eq. (1) is compared above with the splitting estimated from the

TABLE III. Comparison of E_G values.

	E_G (Ry)
Present estimate	0.04
Band calculation (Ref. 7)	0.03
d -state hybridization splitting	< 0.04

band calculation⁷ and with an independent estimate of the coupling between OPW's (orthogonalized plane wave) due to hybridization with the d states.¹² The agreement is satisfactory.

Although only approximate, the result lends itself to a first estimate of the electronic contribution to the ordering energy and is intended as a stimulus for a more careful calculation.

ACKNOWLEDGMENTS

We are pleased to acknowledge helpful discussions at various phases of this work with W. A. Harrison, L. M. Falicov, D. Mikkola, J. McClure, and P. Visscher. This research was supported by the National Science Foundation (Grant No. DMR 78-23011).

¹A. R. von Neida and R. B. Gordon, *Philos. Mag.* **7**, 1129 (1962).

²For a review, see Refs. 10, 11, and references given there.

³For example, Hiroshi Sato and Robert S. Toth, *Phys. Rev. Lett.* **8**, 239 (1962).

⁴M. Sakai and D. E. Mikkola, *Metall. Trans.* **2**, 1635 (1971).

⁵R. C. Kittler and L. M. Falicov, *Phys. Rev. B* **19**, 291 (1979).

⁶For example, J. A. Wilson, F. J. DiSalva, and S. Mahajarn, *Adv. Phys.* **24**, 117 (1975).

⁷H. L. Skriver and H. P. Lengkeek, *Phys. Rev. B* **19**, 900 (1979).

⁸M. R. Halse, *Philos. Trans. R. Soc. London, Ser. A* **265**, 507 (1969).

⁹P. P. Deimel, Ph.D. dissertation (University of Oregon, 1980) (unpublished), available from University Microfilm, Ann Arbor, Michigan. Preliminary reports appeared in *Bull. Am. Phys. Soc.* **25**, 308 (1980); **26**, 236 (1981).

¹⁰P. P. Deimel and R. J. Higgins (unpublished).

¹¹The remarkable closeness is *not* due to residual neck orbits (as from magnetic breakdown through the superlattice gap). The noble-metal neck orbits display quite different angular dependence, which is planned to be discussed elsewhere (Ref. 10).

¹²W. A. Harrison and S. Froyen, *Phys. Rev. B* **21**, 3214 (1980); S. Froyen (private communication) W. A. Harrison (private communication).